Shape-selective diisopropylation of naphthalene in H-Mordenite: Myth or reality?

Christophe Bouvier [a], Wim Buijs [a,*], Jorge Gascon [a], Freek Kapteijn [a], Bogdan C. Gagea [b],
Pierre A. Jacobs [b], Johan A. Martens [b]

[a] Catalysis Engineering, Delft Chem Tech, TU Delft, Julianalaan 136, 2628 BL Delft, The Netherlands
[b] Center for Surface Chemistry and Catalysis, Catholic University of Leuven, Kasteelpark Arenberg 23, Leuven B-3001, Belgium

ARTICLE INFO

ABSTRACT

Selective diisopropylation of naphthalene to 2,6-diisopropylnaphthalene is a challenging goal in sustainable catalysis. Ultrastable Y and H-Mordenite zeolites are the best catalysts reported in the literature with respect to 2,6-diisopropylnaphthalene selectivity. It is generally accepted that in the case of H-Mordenite, shape-selectivity is responsible for the observed 2,6-diisopropylnaphthalene selectivity, while on Ultrastable Y-zeolite, the observed selectivity reflects the internal thermodynamic equilibrium of positional isomers. Revisiting both the experimental and the computational work in this field now leads to the conclusion that shape-selectivity of whatever kind can be ruled out in the case of H-Mordenite. H-Mordenite catalysts produce usually a kinetically controlled mixture of diisopropylnaphthalene isomers which can shift to the direction of a thermodynamical distribution at high reaction temperatures or over more active catalysts.

1. Introduction

Selective diisopropylation of naphthalene to 2,6-diisopropyl-naphthalene (2,6-DIPN) is an important step towards an attractive and sustainable route to 2,6-naphthalene dicarboxylic acid. H-Mordenite and H-USY [1–18] are the best with respect to selectivity, though they largely differ in activity.

Naphthalene dialkylation is a complex reaction. The dialkyl-naphthalenes are prone to many types of reactions such as isomerization, transalkylation and dealkylation [2,19–23].

Shape-selectivity, based on the fit of 2,6-DIPN inside the channel of H-Mordenite, has been widely accepted as the explanation for the high yield to 2,6-DIPN [23]. So far, many research teams have focused on H-Mordenite, its dealuminated versions [1,3,10,24–27], specimens with surface modifications [28–30], as well as on theoretical studies on the isomer formation [19,23,31–36]. At the same time, studies using H-USY [2,4,5,8,13,37] showed even higher yields towards DIPNs in general and 2,6-DIPN particularly.

We were intrigued by the fact that in the case of H-Mordenite, shape-selectivity is used as the dominant explanation for the observed yield, and selectivity while in the case of H-USY thermodynamic control, based on the relative stability of the DIPN isomers,

seems to be the determining factor. This prompted us to reinvestigate the two cases, both experimentally and computationally.

2. Experimental part

2.1. Materials

Naphthalene 98% was purchased from Aldrich, isopropanol (ACS reagent), cyclohexane (99+%) and 2,6-DIPN (99%) were supplied by Acros. All reagents were used without further purification. Commercially available zeolites used were H-USY (CBV760) Si/Al = 30 from PQ and H-MOR Si/Al = 5.9 from Zeocat. H-MOR Si/Al = 24 was synthesized according to the procedure described by Lu et al. [38].

H-MOR 5.9: Crystal size: 0.8–1.0 μm, composition (wt.%): SiO_2: 87.36; Al_2O_3: 12.59; Na_2O: 0.05; Overall atomic Si/Al (chemical composition): 5.9, Framework atomic Si/Al (27Al MAS NMR): 6.9, Crystallinity% (XRD): 97 BET, 500 m^2/g: Bulk density, g/cm^3: 0.63 Brønsted acid site concentration: mmol H+/g of dry zeolite: 1.8.

The acid site concentration was determined using Temperature-Programmed Desorption of ammonia (NH_3-TPD). NH_3-TPD was carried out on a Micromeritics TPR/TPD 2900 apparatus equipped with a thermal conductivity detector (TCD). Approximately, 25 mg of each sample was pretreated at 125 °C and rapidly cooled to 100 °C followed by loading with ammonia applying a flow of 30 mL/min for about 1 h. A He flow of 30 mL/min was applied to remove weakly adsorbed NH_3. A linear temperature program was

started (100–600 °C at 10 °C/min), and the desorbed amount of ammonia was analyzed by the TCD. The TPD spectra were used to analyze the amount of acidic hydroxyl groups present in the catalyst samples.

H-MOR 24: Crystal size: 1.0–1.5 μm, composition (wt%): SiO_2: 87.36; Al_2O_3: 12.59; Na_2O: 0.05; Overall atomic Si/Al (chemical composition): 24, Framework atomic Si/Al (27Al MAS NMR): 20, Crystallinity% (XRD): 98 BET, 546 m^2/g Brønsted acid site concentration: mmol H+/g of dry zeolite: 1.1. A photograph of a typical crystal is shown below in Fig. 1.

2.2. Reaction procedure

Unless mentioned otherwise, all reactions were performed in a 50 mL stainless steel Parr autoclave using the following standard procedure. For alkylation reactions, 320 mg of naphthalene (2.5 mmol), 500 mg of catalyst and 0.38 mL (5.0 mmol) of isopropanol were stirred for 24 h at 200 °C in 25 mL of cyclohexane. At the beginning of a catalytic run, samples were taken hourly. For isomerization reactions, 530 mg of 2,6-DIPN (2.5 mmol) and 500 mg of catalyst in 25 mL of cyclohexane were introduced into the reactor vessel and heated at 200 °C for 24 h. Pressure was built up autogenously. Catalysts were calcined prior to use under an air atmosphere according to the following procedure: 3 °C/min from room temperature to 550 °C and kept at that temperature for 5 h before cooling to room temperature. High amounts of catalyst were used to reach a significant conversion, even with poorly active catalysts. The catalyst was removed from the reaction mixture by filtration over cotton, and the reaction samples were analyzed directly. Generally, mass balances were about 95%. At room temperature, none of the catalysts showed significant preferential absorption of naphthalenic compounds; however, isopropanol was adsorbed up to 25% in H-USY.

2.3. Product analysis

GC × GC analyses were performed using a VF-1 capillary column with dimensions of 50 m × 0.25 mm and film thickness 0.40 μm, combined with a VF-17 capillary column with dimensions 1.5 m × 0.1 mm and film thickness 0.20 μm. Helium was used as carrier gas and the flow was kept constant at 1 mL/min. The split ratio was 1:100. The injection of 1 μl of the sample was performed at 280 °C. The temperature program was as follows: 1 min at 70 °C and a ramp at 5 °C/min till 300 °C. The second dimension time was 2 s and the hot pulse time 0.2 s. GC–MS analyses were performed
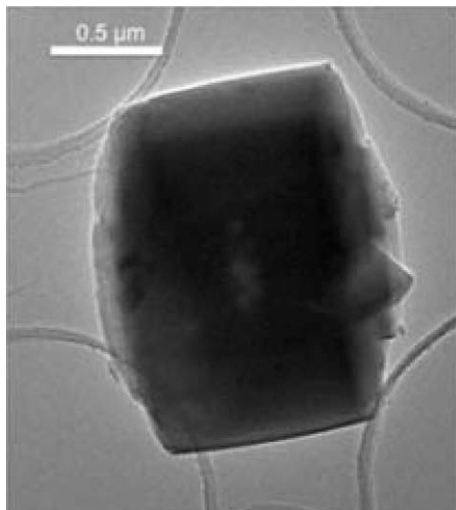

Fig. 1. A typical crystal of H-Mordenite Si/Al = 24.

on a 25 m × 0.25 mm VF-5MS column. Temperature was set at 50 °C for 1 min and then raised till 300 °C at 10 °C/min. Mass spectra were recorded with a VG SE spectrometer at 70 eV. More details about the analytical procedures can be found elsewhere [39].

The following yields and selectivities were calculated based on naphthalene: selectivity towards Naphthalene (N; in isomerization experiments only), IsoPropylNaphthalenes (IPN), DiIsoPropylNaphthalenes (DIPN), PolyIsoPropylNaphthalenes (PIPN), polyalkylated unsaturated compounds (Unsaturates) and Others (not identified naphthalenic compounds). In addition, the isomer distributions in the IPN and DIPN fractions were also determined.

2.4. Molecular modeling

All quantum chemical calculations were carried out using the Spartan '06 molecular modeling suite of programs [40]. First, the most stable DIPN conformers were determined using molecular mechanics (MMFF), next the resulting structures were fully optimized at the B3LYP/6-31G* level, using semi-empirical PM3 data as input. A frequency calculation was performed to allow thermodynamic corrections. Finally, single point calculations on the B3LYP/6-311++G(2df,2p) level were performed on the B3LYP/6-31G* optimized structures. Transition States were fully optimized and checked by animation of their unique imaginary vibration.

3. Results

The consecutive reaction steps in the isopropylation of naphthalene are presented in Fig. 2. Naphthalene with up to 4 isopropyl substituents could be detected in the reaction mixture depending on the reaction conditions. Some polyalkylated unsaturated products (Unsaturates) with mass 252 described by Moreau et al. [5,41] were observed as well.

In close analogy to isobutene [42], isopropanol can be activated by an acidic zeolite to either the isopropyl cation or the isopropyl alkoxide after the elimination of a water molecule. Reaction with naphthalene with the release of a proton leads to an isopropyl naphthalene. Dealkylation can be considered as the reversed reaction. The isopropyl cation can release a proton, leading to the formation of propene. The reaction of propene with an isopropyl moiety is the first step of C_3-oligomerization. Cracking of these C_3-oligomers can occur as well. Reaction products with methyl or ethyl substituents on the naphthalene were detected as well as propene and C_5-alkenes. Evidence for the formation of these light compounds was obtained by leading nitrogen through the reaction mixture. The resulting gas flow was contacted with a solution of bromine in dichloromethane, and the corresponding dibrominated species were identified with GC–MS. Levels were ~0.1% on a molar basis. However, "unsaturates", originating from a C_3-dimer and naphthalene, were present at a detectable level in all experiments and can be considered as an indication for C_3-loss and possibly coke formation.

3.1. Isopropylation of naphthalene and isomerization of 2,6-DIPN over H-USY

Under standard conditions at 200 °C, H-USY showed an excellent 87% conversion already after 4 h, increasing to 91% after 24 h, combined with a yield to DIPNs of 38.4%, and the intermediate IPNs of 37.5%. PIPNs, Unsaturates and Others account for 15% (Fig. 3 and Table 1). Up to 4 h, the (molar) sum of the products and naphthalene was very close to 100%. Later on, the molar sum of identified naphthalene-based reaction products decreased slightly due to the formation of some heavy side products. With respect to the isomeric distribution, in the IPNs, 2-IPN accounted
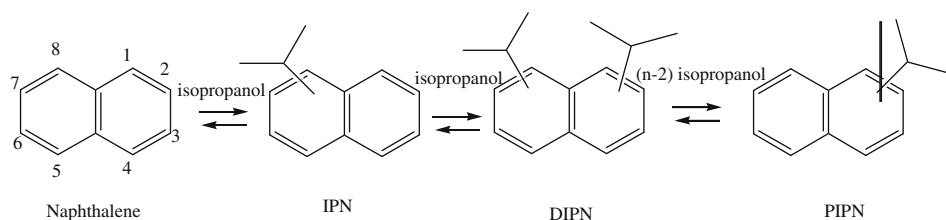
Fig. 2. Consecutive reaction steps in catalytic naphthalene isopropylation.
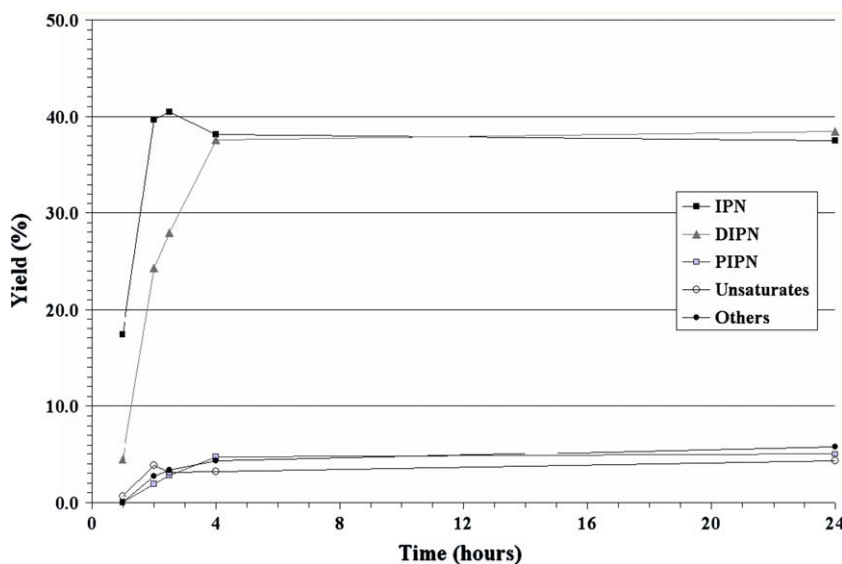

Fig. 3. Yields (%) of various products in the isopropylation of naphthalene over H-USY against reaction time.

for 93% and 1-IPN to 7%. Actually, this resembles the thermodynamic distribution as obtained by computation. In the DIPNs, 2,6-DIPN and 2,7-DIPN accounted for 36% and 42%, respectively.

Table 1 also lists the result of an experiment at 100 °C, sampled after 4 h. The conversion was still 27%, but the product pattern and isomeric distribution of IPNs and DIPNs were completely shifted. The yield to IPNs was 22%, and the yield to DIPNs was 4.3% only. PIPNs, Unsaturates and Others could only be hardly detected. With respect to the isomeric distribution, in the IPNs, 1-IPN accounted

for 72%. In the DIPNs, the α,α-products 1,4-DIPN (33%), and 1,5-DIPN (15.8%) were dominant, followed by α,β-products 1,3-DIPN (11.6%), 1,6-DIPN (12.2%) and 1,7-DIPN (18.9%). β,β-products 2,3-DIPN (3.6%), 2,6-DIPN (3.0%) and 2,7-DIPN (2.4%) were formed only in minor amounts.

Under standard conditions at 200 °C in isomerization, the conversion of 2,6-DIPN reached a maximum of ca. 85% after 4 h and decreased to ca. 81% after 24 h (Table 1 and Fig. 4). The main products were 2-IPN and (non-2,6-) DIPN isomers with yields of 38.9% and 18.2%, respectively, after 24 h. Within isomeric DIPNs, the formation of 2,7-DIPN with a yield of 10.6% was dominant. Product formation in time revealed that naphthalene 2-IPN and 2,7-DIPN were intermediate products in the reaction network. The naphthalene yield showed a minimum of 7.0% after 2 h. 2,6-DIPN showed a weak minimum after 4 h and 2,7-DIPN a distinct maximum of 21.7% after 3 h. It is noteworthy to mention that the highest naphthalene yield (13.0%) was obtained after just 1 h. Thus, dealkylation seems to be the fastest process in the beginning of the reaction. Furthermore, Fig. 4 strongly suggests, by the reciprocal decrease in 2,6-DIPN and increase in 2,7-DIPN, that a transalkylation process contributes to the shift of 2,6- to 2,7-DIPN. In a study to be published separately, more attention will be paid to these kinetic phenomena and the influence of temperature, combined with the results of molecular modeling.

In isomerization, the selectivity to α-substituted products was low. At the end the product distribution showed a striking resemblance with the one obtained in naphthalene isopropylation. Finally, as H-USY remained active over the whole period in both experiments, the level of Unsaturates remained stable after 4 h at ~4.3%, and the overall mass balance was ~95%, coke formation does not seem to be an important factor.

Table 1
Composition of the reaction mixture of the isopropylation of naphthalene, and isomerization of 2,6-DIPN over H-USY after 24 h. Y: yield; ID: isomer distribution.

Catalyst: H-USY	Isopropylation		Isopropylation		Isomerization	
T (°C)	100 (4 h)		200		200	
Compound	Y (%)	ID (%)	Y (%)	ID (%)	Y (%)	ID (%)
Naphthalene	73.2		9.0		9.1	
1-IPN	22.2	72.1	37.5	6.6	38.9	5.1
2-IPN		22.9		93.4		94.9
1,2-DIPN	4.3	0.0	38.4	0.0	37.3	0.0
1,3-DIPN		11.6		5.5		5.7
1,4-DIPN		32.6		0.7		0.8
1,5-DIPN		15.8		2.0		2.0
1,6-DIPN		12.2		5.2		3.2
1,7-DIPN		18.9		4.9		4.8
1,8-DIPN		0.0		0.0		0.0
2,3-DIPN		3.6		3.5		0.1
2,6-DIPN		3.0		36.3		51.2
2,7-DIPN		2.4		42.2		28.3
PIPNs	0.1		5.0		4.4	
Unsaturates	0.1		4.3		4.2	
Others	0.1		5.8		6.1	

3.2. Isopropylation of naphthalene and isomerization of 2,6-DIPN over H-Mordenite

In naphthalene isopropylation over H-Mordenite Si/Al = 5.9, the naphthalene conversion reached ~20% after 20 h in a rather linear way (Fig. 5, Table 2). The main reaction products were 1- and 2-IPN with a total IPN yield of ~17%. The 1-IPN and 2-IPN isomers were present in a ratio close to one. This result can be considered as an indication for a more kinetic product distribution instead of the thermodynamic one obtained with H-USY. The selectivity towards DIPNs was only 1.1%, while PIPNs, Unsaturates and Others accounted only for 0.4%, 1.9% and 0.2%, respectively. Thus, C_3-oligomerization is relatively more prominent compared to DIPN formation as in the case of H-USY, though its absolute level is >2 times lower at 200 °C. However, from the mass balance and the linear growth in time of all products, it might be concluded that coke formation, if significantly present at all, does not seem to play a role in the selectivity pattern obtained under these conditions.

Within the DIPN isomers, the relative yields of 2,6- and 2,7-DIPN were 15% and 10% only. 1,3- 1,4-, 1,5-, 1,6- and 1,7-DIPN account for ~14%, 18%, 9%, 15% and 17%, respectively. From Fig. 5, it is clear that the formation of 1-IPN and 2-IPN, followed by the DIPNs and some side products, remain almost linear in time.

As H-MOR with a Si/Al = 5.9 despite its relative high activity might not be the best candidate to show shape-selectivity, an H-MOR with Si/Al = 24 was used as well. At 200 °C, the decreased acidity and the slightly larger crystal size led to a conversion of ~2% only, and therefore the temperature was raised to 250 °C. At 250 °C, a 4% conversion was reached. The ratio of 2-IPN/1-IPN dropped to 0.5 at 200 °C and 0.6 at 250 °C, compared to 0.9 for H-MOR with Si/Al = 5.9. No major changes were observed in the DIPN isomer distribution. No coke formation was observed, and the mass balance was very close to 100%.

In the isomerization of 2,6-DIPN over H-Mordenite Si/Al = 5.9, a similar ~20% conversion was obtained after 20 h as in the case of diisopropylation. The main reaction products were 2,7-DIPN, 2-
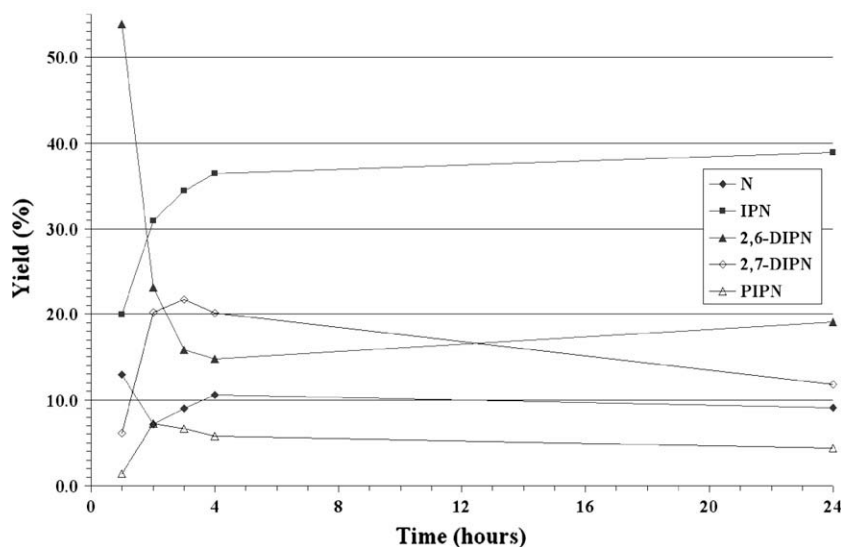

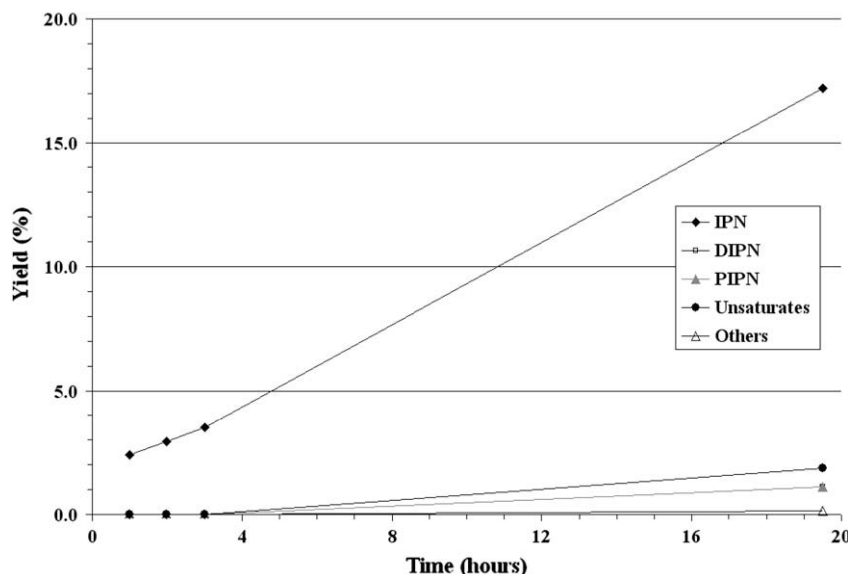**Fig. 4.** Yields (%) of products in the isomerization of 2,6-DIPN over H-USY against time.

Fig. 5. Yields (%) of various products in the isopropylation of naphthalene over H-Mordenite (Si/Al = 5.9) against time.

Table 2
Composition of the reaction product mixture in the isopropylation of naphthalene over H-Mordenite Si/Al = 5.9 and Si/Al = 24, and the isomerization of 2,6-DIPN over H-MOR 5.9. Y: yield; ID: isomer distribution.

Catalyst	H-MOR 5.9		H-MOR 5.9		H-MOR 24			
	Isopropylation		Isomerization		Isopropylation			
T (°C)	200		200		200		250	
Compound	Y (%)	ID (%)	Y (%)	ID (%)	Y (%)	ID (%)	Y (%)	ID (%)
Naphthalene	79.2		2.0		98.4		96.1	
1-IPN	17.2	47.3	5.2	5.1	1.3	67.3	3.5	62.7
2-IPN		52.7		94.9		32.7		37.3
1,2-DIPN	1.1	0.0	91.5	0.0	~0.05	0.0	0.10	0.0
1,3-DIPN		13.6		0.3		14.3		14.7
1,4-DIPN		18.0		0.0		19.7		11.8
1,5-DIPN		8.8		0.0		6.5		5.0
1,6-DIPN		15.5		0.2		19.1		17.1
1,7-DIPN		16.8		0.4		17.5		18.3
1,8-DIPN		0.0		0.0		0.0		0.0
2,3-DIPN		2.1		0.1		1.6		1.3
2,6-DIPN		15.1		89.0		12.8		19.6
2,7-DIPN		10.1		10.2		8.5		12.2
PIPNs	0.4		1.3		<0.01		<0.01	
Unsaturates	1.9		0.0		0.25		0.30	
Others	0.2		0.1		<0.01		<0.01	

IPN, PIPNs and naphthalene with yields of 9.3%, 4.9%, 1.3%, and 2.0%, respectively. Other DIPN isomers besides 2,7-DIPN did appear but in very low amounts. The 2-IPN/1-IPN ratio was close to 20.

Fig. 6 shows a regular build-up in time of most products, except for naphthalene which gave a maximum yield of 5% after 2 h and then gradually decreased to 2%, and 2,6-DIPN which showed a local maximum after 3 h of 95% and then decreased to 81%. This behavior is more or less similar to what was observed with H-USY. Dealkylation seems to be the fastest process in the beginning of the reaction. Transalkylation of 2,6- to 2,7-DIPN seems to play a role also. Whereas in the isopropylation with H-Mordenite Si/Al = 5.9, a significant amount of Unsaturates were formed, in the isomerization of 2,6-DIPN, Unsaturates were not observed at all, but PIPNs were, albeit mainly triisopropylnaphthalenes. Again coke formation was very unlikely.

3.3. Computational results

As mentioned already in the introduction, it is generally accepted that H-USY yields a thermodynamic mixture of DIPN isomers. Table 3 summarizes experimental results with H-USY, H-MOR and computational results using different methods, obtained by other authors and by us.

Experimental values for the DIPN isomer distribution over H-USY are quite similar. The largest difference in the experimental values is ~2.5% for 2,6-DIPN. This is mainly due to our new analytical technique (GC × GC) which allows better peak separation and avoids baseline integration errors which might occur in the older technique [23]. Baseline integration errors lead to a slight overestimation of the large peaks (2,6- and 2,7-DIPN) relative to the smaller peaks of the other DIPN isomers. The computational results obtained with all methods are in quite fair agreement with the experimental data, especially if one takes into account that MP2 results are obtained at 25 °C, B3LYP results at 200 °C and B3PW91 results at 250 °C.

At higher temperature, relative amounts of 2,6- and 2,7-DIPN decrease slightly in favor of other isomers. Both B3LYP and B3PW91 assign 2,7-DIPN as the most abundant isomer in accordance with the experimental data; however, energy differences are so small that no absolute conclusion should be drawn from these findings.

The relative amounts of 1-IPN and 2-IPN are also in agreement with the experimental results obtained with H-USY. Experimentally, distributions of 6.6% and 93.4%, respectively, were found, while 4.5% and 95.5% were calculated.

Furthermore, it should be noted that single point calculations on the B3LYP/6-311++G(2df,2p) level performed on the B3LYP/6-31G* optimized structures did not lead to significantly different results, and these results are therefore not listed.

On the other hand, the isomeric distribution obtained with the H-MOR catalysts seriously deviate from the thermodynamic values. In an attempt to find a possible explanation for these results, electrostatic charges were calculated on different naphthalenic compounds. The results are listed in Table 4.

From Table 4, it is clear that isopropylation of the 1- or α-position of naphthalene is kinetically preferred over the thermodynam-
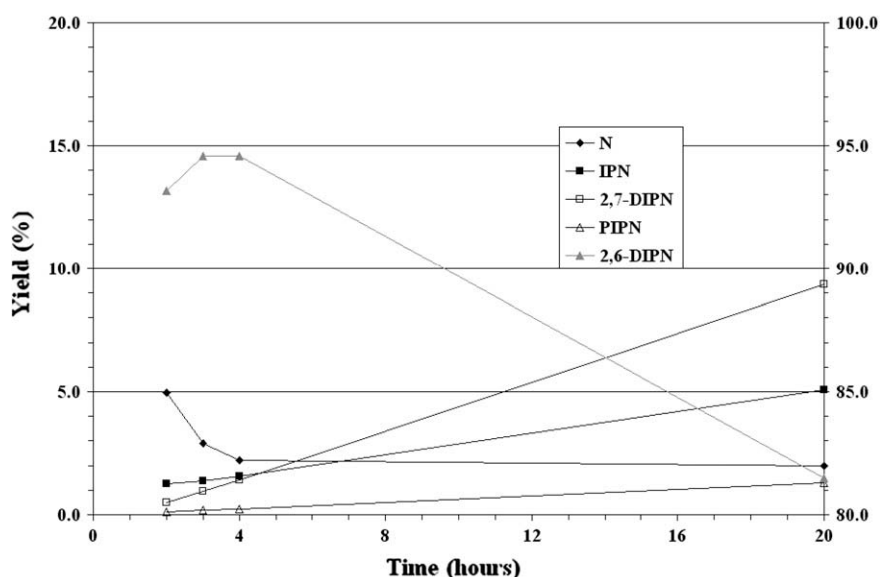

Fig. 6. Yields (%) to various products in the isomerization of 2,6-DIPN over H-Mordenite (Si/Al = 5.9) against time. The amount of 2,6-DIPN relates to the second axis on the right side of the graph.

Table 3
Summary of experimental results on H-USY and H-MOR, and computational results on the thermodynamic equilibrium composition of DIPN isomers.

Compound	Method T (°C)		Catalyst T (°C)	Method T (°C)	Catalyst T (°C)		
	MP2[a] 25	B3LYP[b] 200	H-USY[b] 200	B3PW91[c] 250	H-USY[c] 250	H-MOR 5.9[b] 200	H-MOR 24[b] 250
1,2-DIPN	0.0	0.0	0.0	0.0	0.0	0.0	0.0
1,3-DIPN	2.1	4.0	6.0	5.1	3.8	13.6	14.7
1,4-DIPN	0.0	0.1	0.2	0.5	0.1	18.0	11.8
1,5-DIPN	0.0	0.1	0.2	0.4	0.1	8.8	5.0
1,6-DIPN	1.1	4.5	8.4	5.0	7.6	15.5	17.1
1,7-DIPN	1.7	3.8	4.7	2.5	4.9	16.8	18.3
1,8-DIPN	0.0	0.0	0.0	0.0	0.0	0.0	0.0
2,3-DIPN	0.1	0.3	0.4	1.5	0.4	2.1	1.3
2,6-DIPN	48.7	40.5	37.8	42.0	40.3	15.1	19.6
2,7-DIPN	46.0	46.8	42.4	43.0	42.9	10.1	12.2

[a] Ref. [23].
[b] Our results.
[c] Ref. [19].

ically more stable 2- or β-position, as the negative charge on C_1 is −0.286 vs. −0.094 on C_2. The latter is reflected in the energies of their corresponding Transition States. On the same B3LYP/6-31G* level, the Transition State for the isopropylation at the 1-position of naphthalene lies ∼8 kJ/mol lower as the one for isopropylation at the 2-position. 1-IPN itself shows a kinetic preference for isopropylation at the 4- and 5-position, leading to 1,4- and 1,5-DIPN. 2-IPN shows a kinetic preference for the 4-, 5-, and 8-position, leading to 1,3-, 1,6-, and 1,7-DIPN. Only further net isomerization can lead to the thermodynamically more stable 2,6- and 2,7-DIPN. In a separate experimental and computational study to be reported elsewhere, a more quantitative assessment of the observed DIPN isomer distributions with the various catalysts and temperatures will be presented.

4. Discussion

4.1. Thermodynamic control in H-USY vs. shape-selectivity in H-MOR

For H-USY, Brzozowski et al. [19] showed that the partition of all possible 10 DIPN isomers observed experimentally agreed very well with the one obtained computationally (Table 4. Our isopropylation and isomerization experiments with H-USY, and computational results using standard DFT (B3LYP/6-31G*), fully confirmed the results of Brzozowski et al. Finally, our observed partition of 2- and 1-IPN is also very close to its computed thermodynamic value at 200 °C. Thus, thermodynamic control explains the observed partition of IPN and DIPN isomers, the resulting high selectivity to 2,6- and 2,7-DIPN, and the effect of temperature, very satisfactorily.

H-Mordenite has been used by several authors as catalyst for the diisopropylation of naphthalene [1–3,5,7,9,11,23,26,33,36,43]. Different kinds of shape-selectivity were used to explain the apparent high selectivity to both 2-IPN and 2,6-DIPN.

Moreau et al. [11], under identical experimental conditions as we applied, found that Mordenite catalysts were less active than Y-zeolites. Yields of 2,6- and 2,7-DIPN ranged from 4% to 14% in a ratio ∼1/1 and approaching 80% in the DIPN isomer distribution with Si/Al ranging from 6.9 to 20.6. The relative yield to 2-IPN ranged from ∼55% to 84%. However, all these relative yields to both 2-IPN and 2,6-DIPN are in fact significantly below the yield that would result from a thermodynamic distribution, so there is no reason to use the shape-selectivity argument.

Song et al. [3,33] reported relative high amounts of both 2-IPN, and 2,6-DIPN over Mordenite catalysts with Si/Al ratios ranging from 17 to 35 using decalin and trimethylbenzene as solvents at 250 °C. However, at their highest conversion (28%) in trimethylbenzene, the relative amount of 2-IPN is 89%, still slightly below the thermodynamic value of 95%. Furthermore, the fused silica column applied for their analytics is insufficient to resolve the different DIPN isomers between 41 and 42 min.

Though quite far away from our experimental conditions, Cutrufello et al. [9] revealed the importance of coke formation on the performance of H-MOR in the isopropylation of naphthalene at 350 °C. Conversions decreased from 30% to 20% in time for naphthalene and from 80% to 60% for isopropanol. It was concluded that fast oligomerization of C_3-species and cracking of oligomers caused almost immediate pore blocking, suggesting that the actual isopropylation occurred on or near the outer surface. Their experimental ratio 2-IPN/1-IPN was ∼4, and the DIPN product mixture consisted of ∼8% of 1,3-DIPN, <5% of 1,7-DIPN, <5% of 1,6-DIPN, up to 60% of 2,6-DIPN and up to 30% of 2,7-DIPN. There was a marked influence of on-stream-time on the 2,6-DIPN/2,7-DIPN ratio, starting from ∼1 after 50 min and reaching ∼3 after 350 min. These results cannot be contributed to shape-selectivity as it should be expected that with increasing pore blocking the shape-selective formation of 2,6-DIPN would go down with time on-stream, and the opposite occurs.

Tasi et al. [23] tried to relate the molecular dimensions of the different DIPN isomers to the elliptical main channel size of H-Mordenite (6.5 Å × 7.0 Å) [44]. They stated that 2,6-DIPN (6.61 Å × 6.61 Å) would fit far better as 2,7-DIPN (6.62 Å × 7.26 Å) in the Mordenite main channel. All other DIPN isomers yielded overall much larger dimensions, ranging from 6.22 Å × 9.46 Å for 1,4-DIPN to 6.89 Å × 9.96 Å for 1,3-DIPN. We were able to confirm these molecular dimensions of the isomeric DIPNs, except for 2,7-DIPN, which turned out to be equal to 2,6-DIPN in our hands.

However, contrary to Tasi et al., we state that the sizes of the equilibrium conformers of the different isomers cannot predict the observed isomeric distribution in H-MOR. Except for 2,6-DIPN and 2,7-DIPN, no other isomer should be formed at all, as they are all far too big to fit into the channel. If this approach would be applied to H-USY (7.4 Å × 7.4 Å) [44] also, the isomeric DIPNs, except for 2,6-DIPN and 2,7-DIPN, would not even fit into the faujasite pore entrance. However, even 1,4-DIPN can easily enter the faujasite pore by the rotation of its isopropyl groups, making the molecule much smaller.

In summary, none of these data do support a shape-selectivity explanation. Our computational data both on the thermodynamic DIPN isomer distribution and on the kinetic preferences actually

Table 4
B3LYP/6-31G* calculated electrostatic charges on C_n in naphthalene, 1-IPN and 2-IPN.

Compound	Electrostatic charge on C_n							
	C_1	C_2	C_3	C_4	C_5	C_6	C_7	C_8
Naphthalene	−0.286	−0.094	−0.094	−0.286	−0.286	−0.094	−0.094	−0.286
1-IPN	−0.176	−0.113	−0.109	−0.303	−0.296	−0.073	−0.115	−0.259
2-IPN	−0.485	+0.183	−0.168	−0.287	−0.267	−0.102	−0.104	−0.296

support a rather classical explanation that places the product distributions in between a kinetically and a thermodynamically controlled composition. Our experimental results point into the same direction: the isomeric distributions obtained with H-MOR catalysts are located in between the results obtained with H-USY at 100 °C, yielding a kinetic mixture, and at 200 °C, yielding a thermodynamic mixture. The precise outcome of the different experiments with H-MOR depends on the activity of the catalyst, the temperature (including coke formation and pore blocking) and a minor role of the solvent (cyclohexane, decalin, trimethylbenzene).

Our experimental data are in line with the results of the cited authors, and we do have a more accurate analytical procedure (GC × GC). Routine DFT-calculations support explanations for the catalytic performance of both H-USY and H-MOR based on the normal interplay of thermodynamics and kinetics. The shape-selectivity argument is neither sufficient nor needed to explain our and former experimental data.

5. Conclusions

From all experimental and computational results, it can only be concluded that:

1. H-USY indeed produces a thermodynamic mixture of DIPN isomers, which can be predicted nicely by even routine DFT-calculations. The same calculations also yield qualitative insight in the expected isomeric distribution of DIPN isomers under kinetic conditions, using the electrostatic charges on the relevant carbon atoms.
2. Neither a thermodynamic controlled distribution of DIPN isomers nor a shape-selective one is obtained in the experiments over the various Mordenite catalysts at different temperatures. Arguments against shape-selectivity can be divided into four categories:
   1. There is no reason to use the shape-selectivity argument because the amount of 2,6-DIPN is well below the thermodynamic one, in the presence of high amounts of the other isomers.
   2. The analytical procedure might be insufficient.
   3. Coke formation, leading to pore blocking, actually disables shape-selectivity related to the fit of 2,6-DIPN in the main elliptical channel of H-Mordenite. So, these results cannot be used to advocate shape-selectivity.
   4. Consequences of computational data: the data obtained by Tasi et al. [23] and our data, on the molecular size of all DIPN isomers indicate that apart from 2,6- and 2,7-DIPN no other isomers should be formed if the catalytic reaction would occur in the main channel of H-Mordenite, except for a minor contribution of the outer surface.

We thus conclude that shape-selective formation of 2,6-DIPN in H-MOR is a myth.

3. The actual DIPN mixture obtained with H-MOR catalysts has a distribution in between that of a kinetic and a thermodynamic controlled mixture and is dependent on activity of a specific catalyst, temperature and to some extent of the solvent.

References

[1] C. Song, C.R. Acad. Sci. Paris, Ser. IIc 3 (2000) 477.
[2] Y. Sugi, M. Toba, Catal. Today 19 (1994) 187.
[3] C. Song, S. Kirby, Microporous Mater. 2 (1994) 467.
[4] R. Brzozowski, W. Tecza, Appl. Catal. A 166 (1998) 21.
[5] P. Moreau, C. He, Z. Liu, F. Fajula, J. Mol. Catal. A 168 (2001) 105.
[6] Z. Liu, P. Moreau, F. Fajula, Appl. Catal. A 159 (1997) 305.
[7] A. Katayama, M. Toba, G. Takeuchi, F. Mizukami, S. Niwa, S. Mitamura, J. Chem. Soc., Chem. Commun. 1991 (1991) 39.
[8] S.J. Chu, Y.W. Chen, Appl. Catal. A 123 (1995) 51.
[9] M.G. Cutrufello, I. Ferino, R. Monaci, E. Rombi, V. Solinas, P. Magnoux, M. Guisnet, Appl. Catal. A 241 (2003) 91.
[10] C. Song, Stud. Surf. Sci. Catal. 113 (1998) 163.
[11] P. Moreau, A. Finiels, P. Geneste, J. Solofo, J. Catal. 136 (1992) 487.
[12] Ch. Subrahmanyam, B. Viswanathan, T.K. Varadarajan, J. Mol. Catal. A 226 (2005) 155.
[13] J. Wang, J.-N. Park, Y.-K. Park, C.W. Lee, J. Catal. 220 (2003) 265.
[14] I. Mathew, S. Mayadevi, S. Sabne, S.A. Pardhy, S. Sivasanker, React. Kinet. Catal. Lett. 74 (2001) 119.
[15] I. Mathew, S. Sabne, S. Mayadevi, S.A. Pardhy, S. Sivasanker, Indian J. Chem. Technol. 8 (2001) 469.
[16] G. Kamalakar, S.J. Kulkarni, K.V. Raghavan, S. Unnikrishnan, A.B. Halgeri, J. Mol. Catal. A 149 (1999) 283.
[17] E. Kikuchi, K. Sawada, M. Maeda, T. Matsuda, Stud. Surf. Sci. Catal. 90 (1994) 391.
[18] R. Brzozowski, W. Skupinski, J. Catal. 210 (2002) 313.
[19] R. Brzozowski, J.C. Dobrowolski, M.H. Jamroz, W. Skupinski, J. Mol. Catal. A 170 (2001) 95.
[20] R. Brzozowski, W. Skupinski, J. Catal. 220 (2003) 13.
[21] R. Brzozowski, J. Catal. 232 (2005) 366.
[22] R. Brzozowski, Stud. Surf. Sci. Catal. 158 (2005) 1693.
[23] G. Tasi, F. Mizukami, I. Palinko, M. Toba, A. Kukovecz, J. Phys. Chem. A 105 (2001) 6513.
[24] J.-H. Kim, Y. Sugi, T. Matsuzaki, T. Hanaoka, Y. Kubota, X. Tu, M. Matsumoto, Microporous Mater. 5 (1995) 113.
[25] A.D. Schmitz, C. Song, Catal. Today 31 (1996) 19.
[26] A.D. Schmitz, C. Song, Catal. Lett. 40 (1996) 59.
[27] Y. Sugi, T. Matsuzaki, T. Hanaoka, Y. Kubota, J.-H. Kim, X. Tu, M. Matsumoto, Stud. Surf. Sci. Catal. 90 (1994) 397.
[28] J.-H. Kim, Y. Sugi, T. Matsuzaki, T. Hanaoka, Y. Kubota, X. Tu, M. Matsumoto, S. Nakata, A. Kato, Appl. Catal. A 131 (1995) 15.
[29] Y. Sugi, K. Nakajima, S. Tawada, J.-H. Kim, T. Hanaoka, T. Matsuzaki, Y. Kubota, K. Kunimori, Stud. Surf. Sci. Catal. 125 (1999) 359.
[30] Y. Sugi, J.-H. Kim, T. Matsuzaki, T. Hanaoka, Y. Kubota, X. Tu, M. Matsumoto, Stud. Surf. Sci. Catal. 84 (1994) 1837.
[31] P. Moreau, Z. Liu, F. Fajula, J. Joffre, Catal. Today 60 (2000) 235.
[32] G. Tasi, I. Palinko, F. Mizukami, React. Kinet. Catal. Lett. 74 (2001) 317.
[33] C. Song, X. Ma, H.H. Schobert, ACS Symp. Ser. 738 (2000) 305.
[34] C. Song, X. Ma, A.D. Schmitz, H.H. Schobert, Appl. Catal. A 182 (1999) 175.
[35] J.A. Horsley, J.D. Fellmann, E.G. Derouane, C.M. Freeman, J. Catal. 147 (1994) 231.
[36] G. Tasi, F. Mizukami, M. Toba, S. Niwa, I. Palinko, J. Phys. Chem. A 104 (2000) 1337.
[37] P. Moreau, A. Finiels, P. Geneste, F. Moreau, J. Solofo, Stud. Surf. Sci. Catal. 78 (1993) 575.
[38] B. Lu, T. Tsuda, Y. Oumi, K. Itabashi, T. Sano, Microporous Mesoporous Mater. 76 (2004) 1.
[39] C. Bouvier, N. Reumkens, W. Buijs, J. Chromatogr. A 1216 (2009) 6410.
[40] Wavefunction, Inc., 18401 Von Karman Avenue, Suite 370, Irvine, CA 92612, USA.
[41] C. He, Z. Liu, F. Fajula, P. Moreau, Chem. Commun. 18 (1998) 1999.
[42] C. Tuma, J. Sauer, Angew. Chem. 117 (2005) 2.
[43] P. Moreau, A. Finiels, P. Geneste, J. Joffre, F. Moreau, J. Solofo, Catal. Today 31 (1996) 11.
[44] Database of zeolite structures. Choose MOR (FAU) in the table of frameworks, and next select Type Material to yield the channel dimensions. <http://www.iza-structure.org/databases/>.